

# Mathematical aspects of vacuum energy on quantum graphs

G Berkolaiko<sup>1</sup>, J M Harrison<sup>1,2</sup> and J H Wilson<sup>1,3</sup>

<sup>1</sup> Dept. of Mathematics, Texas A&M University, College Station, TX 77843-3368, USA

<sup>2</sup> Department of Mathematics, Baylor University, Waco, TX 76798, USA

<sup>3</sup> University of Maryland, Department of Physics, College Park, MD 20742, USA

E-mail: gregory.berkolaiko@math.tamu.edu, jon\_harrison@baylor.edu,  
jwilson.thequark@gmail.com

**Abstract.** We use quantum graphs as a model to study various mathematical aspects of the vacuum energy, such as convergence of periodic path expansions, consistency among different methods (trace formulae versus method of images) and the possible connection with the underlying classical dynamics. In our study we derive an expansion for the vacuum energy in terms of periodic paths on the graph and prove its convergence and smooth dependence on the bond lengths of the graph. For an important special case of graphs with equal bond lengths, we derive a simpler explicit formula. With minor changes this formula also applies to graphs with rational (up to a common factor) bond lengths. The main results are derived using the trace formula. We also discuss an alternative approach using the method of images and prove that the results are consistent. This may have important consequences for other systems, since the method of images, unlike the trace formula, includes a sum over special “bounce paths”. We succeed in showing that in our model bounce paths do not contribute to the vacuum energy. Finally, we discuss the proposed possible link between the magnitude of the vacuum energy and the type (chaotic vs. integrable) of the underlying classical dynamics. Within a random matrix model we calculate the variance of the vacuum energy over several ensembles and find evidence that the level repulsion leads to suppression of the vacuum energy.

AMS classification scheme numbers: 34B45, 81Q10, 15A52

## 1. Introduction

Vacuum energy is a concept arising in quantum field theory and was first shown by Casimir [1] to have an observable effect on two perfectly conducting parallel plates, causing them to attract. Since then, experiments with various physical geometries have confirmed the effects of vacuum energy (see [2, 3, 4, 5]).

In time-independent situations the vacuum energy is formally given by

$$E = \frac{1}{2} \sum_n k_n \tag{1}$$

where  $k_n^2$  are the eigenvalues of a Hamiltonian,  $H$ , where throughout we take  $\hbar = 1 = c$ . The above expression arises in quantum field theory in the context of cavities and cosmological models [3], and it is formally divergent. To get meaningful result from this expression, the vacuum energies for two different configurations are subtracted from one another [2]. To accomplish this in a systematic way, we employ an ultra-violet cutoff defining the energy as the regular part of

$$E(t) = \frac{1}{2} \sum_n k_n e^{-k_n t}, \tag{2}$$

as  $t \rightarrow 0$ . To evaluate (2), it is sometimes convenient to employ the trace of the cylinder kernel,  $T(t) = \sum_n e^{-k_n t}$ , [6]. In this way,  $E(t) = -T'(t)/2$ . The singular term in the expansion of  $E(t)$  is related to the vacuum energy density of free space, and physical justification for its removal is described, for example, in [2] (for systems similar to those considered here, see [7, 8]).

A widely employed method of calculation of the vacuum energy is expanding it into a sum over classical paths [9, 10, 11, 12, 13, 14]. The expansion is usually done by the method of images, or “multiple reflections”, leading to a sum over all closed paths. It has been argued in [11] that for certain geometries restricting the sum to include only the periodic paths (“semiclassical evaluation”) correctly reproduces asymptotic behavior of the vacuum energy and is much simpler to evaluate. A periodic path comes back to the starting point with the same momentum, while a closed path might not. Another popular approximation predicts the sign of the vacuum energy by considering only short orbits [15, 8]. This implicitly assumes that the convergence of the complete series is sufficiently fast.

In the present paper we aim to contribute to this discussion by studying the vacuum energy on quantum graphs (for another model where similar questions are addressed, see [16]) . Quantum graphs are often used as mathematical models that exhibit the relevant phenomena while being sufficiently simple to allow mathematical treatment. We compare the method of images with the direct application of the trace formula (which is exact on graphs) and demonstrate that the outcome is the same. This is done by showing that the contribution of the “bounce paths” — the paths that are closed but not periodic — is

identically zero. We also prove that the resulting sums converge, giving an estimate for the rate of convergence, and can be differentiated term-by-term with respect to the topological parameters present in the model.

One of the main reasons for the success of quantum graphs as models (for example, of quantum chaos, see [17] for a review) is the existence of an exact trace formula on quantum graphs. A trace formula is a relation between the spectrum and the set of periodic orbits of the system. For graphs, the trace formula was first found by Roth [18] and then by Kottos and Smilansky [19]. Subsequent studies of the mathematical properties of the trace formula on graphs included works by Kostrykin, Potthoff and Schrader [20] and Winn [21].

The trace formula of [19] gives an expression for the density of states  $d(k)$  defined as

$$d(k) = \sum_{n=1}^{\infty} \delta(k - k_n), \quad (3)$$

where  $\delta(\cdot)$  is the Dirac delta-function. The vacuum energy is then, formally,

$$E(t) = \frac{1}{2} \int k e^{-kt} d(k) dk, \quad (4)$$

quickly leading to the result (for  $k$ -independent scattering matrices, see Sec. 2),

$$E_c = -\frac{1}{2\pi} \sum_{n=1}^{\infty} \sum_{p \in \mathcal{P}} \frac{A_p}{\ell_p n_p}. \quad (5)$$

The sum is over the set of all periodic paths  $\mathcal{P}$  on the graph,  $\ell_p$  is the metric length of the path  $p$ ,  $n_p$  is the period (the number of bonds) of the path and  $A_p$  is its stability amplitude (see Section 4.1 for definitions).

After introducing the notation in Section 2 and considering some explicit examples in Section 3, we prove the mathematical correctness of the calculation outlined above. This is done in Section 4.3, where the convergence of (5) is also analyzed. In Section 4.4 we show that we can differentiate (5) with respect to individual bond lengths, showing the smoothness ( $C^\infty$ ) of  $E_c$  as a function of lengths.

In Section 5 we briefly discuss the method of images (covered more fully in [22]) and show that the contributions from the bounce paths cancel. Finally, in Section 6.1 we discuss random matrix models of the vacuum energy. As expected, in such models the average vacuum energy is zero and there is no preferred sign to the Casimir force. However, by analyzing the second moment of the energy we confirm an earlier observation by Fulling [23, 6] that level repulsion tends to decrease the *magnitude* of the energy.

## 2. Vacuum energy and quantum graphs

Quantum graphs were introduced as a model of vacuum energy by Fulling [24] who considered the effect of the energy density near a quantum graph vertex by constructing the cylinder

kernel for an infinite star graph (a graph with one vertex and  $B$  bonds extending to infinity). The quantum field theory origins of this in a graph context were given by Bellazzini and Mintchev [25]. The vacuum energy expression for quantum graphs obtained in the present manuscript was also used in [8] where the convergence was investigated numerically (we prove rigorous estimates here).

We start by briefly recalling the terminology of the quantum graph model, see [26] for a general review of quantum graphs. We consider a finite metric graph  $\Gamma$  consisting of a set of vertices  $\mathcal{V}$ , and a set of bonds  $\mathcal{B}$ . A (undirected) bond  $b$  connecting the vertices  $v$  and  $w$  is denoted by  $\{v, w\}$ . Each bond  $b$  is associated with a closed interval  $[0, L_b]$ , thus fixing a preferred direction along the bond (from 0 to  $L_b$ ). This direction can be chosen arbitrarily. If the direction from  $v$  to  $w$  is chosen, the bond  $b = \{v, w\}$  gives rise to two directed bonds,  $b^+ = (v, w)$  and  $b^- = (w, v)$ . Whenever the distinction between  $b^+$  and  $b^-$  is unimportant, we will denote the directed bonds by Greek letters:  $\alpha, \beta$ . In addition, the reversal  $\alpha$  is denoted by  $\bar{\alpha}$  (e.g. if  $\alpha = b^+$ , then  $\bar{\alpha} = b^-$ ). We will denote by  $B$  the number of bonds  $|\mathcal{B}|$ ; correspondingly, the number of directed bonds is  $2B$ . The length of the directed bond is naturally determined by the length  $L_b$  of the underlying undirected bond. The total length of  $\Gamma$  is  $\mathcal{L} = \sum_{b \in \mathcal{B}} L_b$ . We will denote by  $\mathbf{L} = \text{diag}\{L_1, \dots, L_B, L_1, \dots, L_B\}$  the diagonal  $2B \times 2B$  matrix of directed bond lengths.

In this article we study the spectrum of the negative Laplacian on the graph. The Laplacian acts on the Hilbert space  $\mathcal{H}(\Gamma) := \bigoplus_{b \in \mathcal{B}} H^2([0, L_b])$  of (Sobolev) functions defined on the bonds of the graph. On the bond  $b$  it acts as the 1-dimensional differential operator  $-\frac{d^2}{dx_b^2}$ . A domain on which the Laplacian is self-adjoint may be defined by specifying matching conditions at the vertices of  $\Gamma$ , see e.g. [27, 28, 29, 26].

To specify the matching conditions, let  $f$  be a function in  $\mathcal{H}(\Gamma)$ . For a vertex  $v$  of degree  $d$  we denote by  $\mathbf{f}^{(v)}$  the vector of values of  $f$  at  $v$ ,  $\mathbf{f}^{(v)} = (f_{b_1}(v), \dots, f_{b_d}(v))^T$ , where  $f_b(v) = f_b(0)$  if  $b = \{v, w\}$  is oriented from  $v$  to  $w$  and  $f_b(v) = f_b(L_b)$  otherwise. Furthermore, let  $\mathbf{g}^{(v)}$  denote the vector of outgoing derivatives of  $f$  at  $v$ ,  $\mathbf{g}^{(v)} = (f'_{b_1}(v), \dots, f'_{b_d}(v))^T$ , i.e.  $f'_b(v) = f'_b(0)$  if  $b = \{v, w\}$  is oriented from  $v$  to  $w$  and  $f'_b(v) = -f'_b(L_b)$  otherwise. Matching conditions at  $v$  can be specified by a pair of matrices  $\mathbb{A}^{(v)}$  and  $\mathbb{B}^{(v)}$  through the linear equation

$$\mathbb{A}^{(v)} \mathbf{f}^{(v)} + \mathbb{B}^{(v)} \mathbf{g}^{(v)} = \mathbf{0} . \quad (6)$$

The matching conditions define a self-adjoint operator if  $(\mathbb{A}^{(i)}, \mathbb{B}^{(i)})$  has maximal rank and  $\mathbb{A}^{(i)} \mathbb{B}^{(i)\dagger}$  is self-adjoint at each vertex (where a  $\mathbb{B}^{(i)\dagger}$  represents the adjoint of  $\mathbb{B}$ ).

A solution to the eigenvalue equation on the bond  $b$ ,

$$-\frac{d^2}{dx_b^2} \psi_b(x_b) = k^2 \psi_b(x_b), \quad (7)$$

can be written as a linear combination of plane waves,

$$\psi_b(x_b) = c_b e^{ikx_b} + \hat{c}_b e^{-ikx_b} . \quad (8)$$

where  $c$  is the coefficient of an outgoing plane wave at 0 and  $\hat{c}$  the coefficient of the incoming plane wave at 0. A solution on the whole graph can be defined by specifying the corresponding vector of coefficients  $\mathbf{c} = (c_1, \dots, c_B, \hat{c}_1, \dots, \hat{c}_B)^T$ .

The matching conditions at the vertex  $v$  define a vertex scattering matrix

$$\boldsymbol{\sigma}^{(v)}(k) = -(\mathbb{A}^{(v)} + ik\mathbb{B}^{(v)})^{-1}(\mathbb{A}^{(v)} - ik\mathbb{B}^{(v)}), \quad (9)$$

see [27].  $\boldsymbol{\sigma}^{(v)}$  is unitary and the elements of  $\boldsymbol{\sigma}^{(v)}$  are complex transition amplitudes which in general depend on  $k$ . However, for a large class of matching conditions including the so called Kirchhoff or natural conditions the S-matrix is independent of  $k$ . Kirchhoff matching conditions require that  $\psi$  is continuous at the vertex and the outgoing derivatives of  $\psi$  at the vertex sum to zero. These conditions may be written in the form (6) with matrices

$$\mathbb{A} = \begin{pmatrix} 1 & -1 & 0 & 0 & \dots \\ 0 & 1 & -1 & 0 & \dots \\ & & \ddots & \ddots & \\ 0 & \dots & 0 & 1 & -1 \\ 0 & \dots & 0 & 0 & 0 \end{pmatrix} \quad \mathbb{B} = \begin{pmatrix} 0 & 0 & \dots & 0 \\ \vdots & \vdots & & \vdots \\ 0 & 0 & \dots & 0 \\ 1 & 1 & \dots & 1 \end{pmatrix}. \quad (10)$$

Substituting in (9) leads to  $k$ -independent transition amplitudes

$$[\boldsymbol{\sigma}]_{ij} = \frac{2}{d} - \delta_{ij}, \quad (11)$$

where  $d$  is the degree of  $v$ .

The matrix  $\boldsymbol{\sigma}^{(v)}$  relates incoming and outgoing plane wave coefficients at  $v$ ,  $\mathbf{c}^{(v)} = \boldsymbol{\sigma}\hat{\mathbf{c}}^{(v)}$ . Collecting together transition amplitudes from all the vertices of a graph we may define the familiar  $2B \times 2B$  *bond scattering matrix*  $\mathbf{S}$  [30],

$$[\mathbf{S}]_{(v',w')(v,w)} = \delta_{w,v'}[\boldsymbol{\sigma}^{(w)}]_{(v,w)}. \quad (12)$$

We shall also need the *quantum evolution operator*  $\mathbf{U} = \mathbf{S}e^{ik\mathbf{L}}$ , which acts on the vector of  $2B$  plane wave coefficients indexed by directed bonds. For a general graph, the spectrum can be computed as the zeros of the equation

$$\det(\mathbf{I} - \mathbf{S}e^{ik\mathbf{L}}) = 0. \quad (13)$$

This formula goes back at least to [31]; for a discussion of scattering matrices of different types we refer the reader to [30].

The spectral theory of quantum graphs is often extended to included quantum evolution operators defined by specifying *a priori* a set of unitary vertex scattering matrices as in [32, 33]. The vertex scattering matrices are typically chosen to be  $k$  independent and to have other desirable features, for instance transition amplitudes of equal magnitude as is the case if the scattering matrix is a fast Fourier transform matrix

$$[\boldsymbol{\sigma}]_{ij} = \frac{1}{\sqrt{d}}e^{i\frac{2\pi}{d}ij}. \quad (14)$$

Such a scattering matrix would be difficult to produce from matching conditions of a self-adjoint operator at a vertex. For such a quantum evolution operator the spectrum is still defined by (13) however the scattering matrices in general no longer correspond to a self-adjoint realization of the Laplace operator on the graph.

In the following we work with  $k$ -independent scattering matrices which can either be considered to come from a self-adjoint Laplace operator or through specifying unitary vertex scattering matrices directly.

### 3. Some explicit examples

#### 3.1. Star graph with bonds of equal length

One case where the vacuum energy can be computed explicitly is the quantum star graph with bonds of equal length. This example was first considered in [8] and here, for completeness, we summarize the computation.

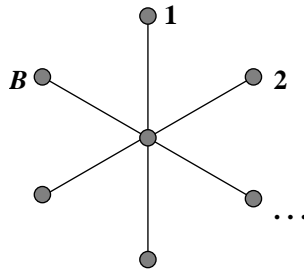


**Figure 1.** A star graph with  $B$  bonds

Consider a star graph (see Fig. 1) with  $B$  bonds. The bond  $b$  has length  $L_b$ . We consider the equation (7) with Neumann conditions. At the central vertex, this translates into

$$\sum_b \psi'_b(0) = 0, \quad \psi_1(0) = \dots = \psi_B(0) \quad (15)$$

and, at the end-vertices, into

$$\psi'_b(L_b) = 0, \quad \forall b. \quad (16)$$

Solutions of (7) together with (16) can be written as

$$\psi_b(x) = C_b \cos(k(L_b - x)).$$

Imposing (15) we conclude that the spectrum consists of the solutions to

$$Z(k) = \sum_{b=1}^B \tan(kL_b) = 0,$$

if the lengths are rationally independent. We note that since  $Z(k)$  is an increasing function, there is exactly one zero of  $Z(k)$  between each pair of consecutive poles. Because of rational independence, the poles of different tangents do not coincide. If we lift the restriction on lengths, in addition to the zeros of  $Z(k)$  we have the following eigenvalues:  $\kappa$  is an eigenvalue of multiplicity  $m$  if there are  $m + 1$  lengths  $L_{b_j}$  such that  $\kappa$  is a pole of each  $\tan(kL_{b_j})$ .

In particular, if all lengths are equal,  $L_1 = \dots = L_B = L$ ,  $Z(k)$  is simply  $B \tan(kL)$ . Each zero of  $Z(k)$  is a simple eigenvalue, while each pole is an eigenvalue of multiplicity  $B - 1$ . We can now evaluate

$$\begin{aligned} T(t) &= \sum_{n=1}^{\infty} e^{-tk_n} = \sum_{n=0}^{\infty} e^{-n\pi t/L} + (B-1) \sum_{n=0}^{\infty} e^{-(2n+1)\pi t/2L} = \frac{1 + (B-1)e^{-\pi t/2L}}{1 - e^{-\pi t/L}} \\ &= \frac{BL}{\pi} t^{-1} + \frac{1}{2} - \frac{(B-3)\pi}{24L} t + O(t^2) \end{aligned}$$

Now we take the regular part and the limit  $t \rightarrow 0$  of  $-T'(t)/2$  which gives us the vacuum energy,

$$E_c = \frac{(B-3)\pi}{48L}. \quad (17)$$

### 3.2. General graphs with bonds of equal length

If all bond lengths of the graph are equal to  $L$ , we can use equation (13) to explicitly describe the infinite spectrum of the graph in terms of the finite spectrum of  $\mathbf{S}$ . Indeed let  $\mathbf{\Lambda}$  be the diagonal matrix of the eigenvalues of  $\mathbf{S}$ . Then  $e^{ik\mathbf{L}} = e^{ikL}\mathbf{I}$  and, therefore,  $\det(\mathbf{I} - \mathbf{S}e^{ikL\mathbf{I}}) = \det(\mathbf{I} - \mathbf{\Lambda}e^{ikL})$ . Consequently the solutions of equation (13) are the values  $k$  such that

$$e^{ikL}e^{i\theta_j} = 1 \quad (18)$$

for some  $j$ . Here by  $e^{i\theta_j}$  we denoted the  $j$ -th eigenvalue of (unitary) matrix  $\mathbf{S}$ . Thus the  $k$ -spectrum is

$$\bigcup_{j=1}^{2B} \left\{ \frac{2\pi n - \theta_j}{L} \right\}_{n=1}^{\infty} \quad (19)$$

where we choose  $\theta_j$  to lie between 0 and  $2\pi$ .

Now we compute the trace of the cylinder kernel  $T(t)$

$$T(t) = \sum_{n=1}^{\infty} e^{-tk_n} = \sum_{j=1}^{2B} e^{t\theta_j/L} \sum_{n=1}^{\infty} e^{-2\pi n t/L} = (e^{2\pi t/L} - 1)^{-1} \sum_{j=1}^{2B} e^{t\theta_j/L} \quad (20)$$

$$= \sum_{j=1}^{2B} \left[ \frac{L}{2\pi t} + \frac{\theta_j - \pi}{2\pi} + \frac{3\theta_j^2 + 2\pi^2 - 6\theta_j\pi}{12L\pi} t + O(t^2) \right]. \quad (21)$$

Thus, the vacuum energy is

$$E_c = - \sum_{j=1}^{2B} \frac{3\theta_j^2 + 2\pi^2 - 6\theta_j\pi}{12L\pi} = -\frac{\pi}{L} \sum_{j=1}^{2B} B_2(\theta_j/2\pi), \quad (22)$$

where  $B_2(\cdot)$  is the second Bernoulli polynomial (compare to the  $B = 1$  case discussed in [6]).

As an example of application of formula (22) consider again the star graph with equal bond lengths. The eigenphases  $\theta_j$  of the S-matrix of a star graph are  $0, \pi, \pi/2$  and  $3\pi/2$ , the latter two with multiplicity  $B - 1$ . Substituting into equation (22) one can recover (17).

### 3.3. Graphs with bonds of rational length

By introducing the Neumann vertices of degree 2 we do not change the spectrum of the graph and therefore the vacuum energy. On the other hand, if the bonds of the graph are rational (up to an overall factor), by introducing such “dummy” vertices we can convert the original graph into a graph with bonds of equal length. The number of bonds (and the dimension of the scattering matrix  $\mathbf{S}$ ) will increase as a result, but the vacuum energy will still be explicitly computable using equation (22).

Moreover, one can conceivably approximate rationally independent lengths by rational ones and use the result as a numerical approximation to the true vacuum energy. For this approach to work one needs to know, *a priori*, that  $E_c$  is continuous as a function of bond lengths. This question is one of the main subjects of Section 4.

## 4. Vacuum energy via the trace formula

### 4.1. Formal calculation

In this section we perform a formal calculation of the vacuum energy  $E_c$  using the trace formula. We shall investigate the rigor of the manipulations in Section 4.3.

The trace formula (see, e.g. [17]) connects the spectrum  $\{k_n\}$  of the graph with the set of all periodic orbits (or periodic paths) on the graphs. A periodic path of period  $n$  is a sequence  $(\alpha_1, \alpha_2, \dots, \alpha_n)$  of directed bonds which satisfy  $[\mathbf{S}]_{\alpha_{j+1}, \alpha_j} \neq 0$  for all  $j = 1, \dots, n$  (the index  $j + 1$  is taken modulo  $n$ ). A periodic orbit is an equivalence class of periodic paths with respect to the cyclic shift  $(\alpha_1, \alpha_2, \dots, \alpha_n) \mapsto (\alpha_2, \dots, \alpha_n, \alpha_1)$ . We denote by  $\mathcal{P}_n$  the set of all periodic paths of period  $n$  and by  $\mathcal{P}$  the set of periodic paths of all periods. The trace formula can be written as

$$d(k) \equiv \sum_{n=1}^{\infty} \delta(k - k_n) = \frac{\mathcal{L}}{\pi} + \frac{1}{\pi} \text{Re} \sum_{p \in \mathcal{P}} A_p \frac{\ell_p}{n_p} e^{ik\ell_p}, \quad (23)$$

where  $\mathcal{L}$  is the total length of the graph (the sum of the bond lengths),  $n_p$  is the period of the periodic path  $p$ ,  $\ell_p = \sum_{j=1}^{n_p} L_{\alpha_j}$  is the length of  $p$  and  $A_p = \prod_{j=1}^{n_p} [\mathbf{S}]_{\alpha_{j+1}, \alpha_j}$  is its



amplitude. Using the trace formula and equation (2) we can formally compute the vacuum energy. Indeed,

$$\sum_{n=1}^{\infty} k_n e^{-tk_n} = \int_0^{\infty} k e^{-kt} d(k) dk \quad (24)$$

$$= \frac{\mathcal{L}}{2\pi} \int_0^{\infty} k e^{-kt} dk + \frac{1}{\pi} \operatorname{Re} \sum_{p \in \mathcal{P}} A_p \frac{\ell_p}{n_p} \int_0^{\infty} k e^{-kt + ik\ell_p} dk \quad (25)$$

$$= \frac{\mathcal{L}}{\pi} t^{-2} + \frac{1}{\pi} \operatorname{Re} \sum_{p \in \mathcal{P}} \frac{A_p \ell_p}{n_p (t - i\ell_p)^2} \quad (26)$$

Removing the divergent Weyl term  $\mathcal{L}/\pi t^2$  due to regularization and taking the limit  $t \rightarrow 0$  leads to the following simple expression for the vacuum energy,

$$E_c = -\frac{1}{2\pi} \operatorname{Re} \sum_{p \in \mathcal{P}} \frac{A_p}{\ell_p n_p}. \quad (27)$$

#### 4.2. Equal bond lengths; equivalence to (22)

In the case of equal bond lengths (27) should be equivalent to the sum of second Bernoulli polynomials (22). If the length of each bond is  $L$  an orbit that visits  $n$  bonds has length  $nL$  and we may rewrite (27) as a sum over the topological length  $n$  followed by a sum over the set of all periodic paths visiting  $n$  bonds,  $\mathcal{P}_n$ ,

$$E_c = -\frac{1}{2\pi L} \operatorname{Re} \sum_{n=1}^{\infty} \frac{1}{n^2} \sum_{p \in \mathcal{P}_n} A_p \quad (28)$$

$$= -\frac{1}{2\pi L} \sum_{n=1}^{\infty} \frac{1}{n^2} \sum_{\alpha_1=1}^{2B} \dots \sum_{\alpha_n=1}^{2B} \operatorname{Re}(S_{\alpha_1 \alpha_2} S_{\alpha_2 \alpha_3} \dots S_{\alpha_n \alpha_1}) \quad (29)$$

$$= -\frac{1}{2\pi L} \sum_{n=1}^{\infty} \frac{1}{2n^2} (\operatorname{tr} \mathbf{S}^n + \operatorname{tr}(\mathbf{S}^\dagger)^n) \quad (30)$$

$$= -\frac{1}{2\pi L} \sum_{n=1}^{\infty} \sum_{j=1}^{2B} \frac{\cos n\theta_j}{n^2}, \quad (31)$$

where  $e^{i\theta_j}$  are the eigenvalues of the matrix  $\mathbf{S}$  with  $0 \leq \theta \leq 2\pi$ . The sum over  $n$  can be expressed in a closed form, see Abramowitz and Stegun [34], formulae 27.8.6,

$$\sum_{n=1}^{\infty} \frac{\cos(n\theta)}{n^2} = \frac{3\theta^2 + 2\pi^2 - 6\pi\theta}{12} = \pi^2 B_2(\theta/2\pi), \quad (32)$$

where  $B_2(\cdot)$  is the second Bernoulli polynomial. Consequently we recover expression (22).

### 4.3. Convergence of (27); vacuum energy as a function of the bond lengths

We shall now present a rigorous derivation of equation (27).

**Theorem 1.** *The vacuum energy of the graph, defined as*

$$E_c = \frac{1}{2} \lim_{t \rightarrow 0^+} \left[ \sum_{n=1}^{\infty} k_n e^{-tk_n} - \frac{\mathcal{L}}{\pi t^2} \right],$$

is given by

$$E_c = \frac{1}{2\pi} \sum_{n=1}^{\infty} \frac{1}{n} \operatorname{Re} \int_0^{\infty} \operatorname{tr} (\mathbf{S} e^{-s\mathbf{L}})^n ds \quad (33)$$

$$= -\frac{1}{2\pi} \operatorname{Re} \sum_{n=1}^{\infty} \sum_{p \in \mathcal{P}_n} \frac{A_p}{\ell_p n_p}, \quad (34)$$

where  $\mathcal{P}_n$  denotes the set of all periodic paths of period  $n$ . The vacuum energy is smooth ( $C^\infty$ ) as a function of bond lengths on the set  $\{L_b > 0\}$ .

**Remark 1.** The sum over the periodic orbits in (34) is finite for each  $n$ . We will show, in particular, that the sum over  $n$  is absolutely and uniformly convergent. More precisely we will derive the following bound,

$$\left| \sum_{p \in \mathcal{P}_n} \frac{A_p}{\ell_p n} \right| \leq \frac{2B}{n^2 L_{\min}}, \quad (35)$$

where  $2B$  is the number of (directed) bonds and  $L_{\min}$  is the minimal bond length. This estimate shows that, if the (finite!) sum over periodic orbits of a fixed length is performed first, the series in (34) becomes absolutely convergent. Moreover, it is uniformly convergent with respect to the change in bond length as long as  $L_{\min}$  remains bounded away from zero.

We would like to mention that our estimate (35) agrees with the numerical results of [8], even though in [8] the ordering of the periodic orbits was different (according to the metric length  $\ell_p$  rather than topological length  $n$ ).

*Proof of (33)-(34).* The  $C^\infty$  part of the proof will be given in the following section.

We start with the definition of the vacuum energy and integrate by parts,

$$\sum_{n=1}^{\infty} k_n e^{-tk_n} = \int_0^{\infty} (tk - 1) e^{-tk} N(k) dk, \quad (36)$$

where  $N(k)$  is the *integrated density of states* (IDS), a piecewise constant, increasing function

$$N(k) = \#\{n : 0 < k_n < k\}. \quad (37)$$

The integrated density of states  $N(k)$  can be split into two parts,

$$N(k) = \operatorname{const} + \frac{k\mathcal{L}}{\pi} + N^{\operatorname{osc}}(k). \quad (38)$$

The first two terms are unimportant: The first term makes no contribution in the integral, and the second term is removed at the regularization stage. The oscillatory part possesses an expansion, see [17], equation (5.24),

$$N^{\text{osc}}(k + i\varepsilon) = \frac{1}{\pi} \text{Im} \sum_{n=1}^{\infty} \frac{1}{n} \text{tr} \mathbf{U}^n(k + i\varepsilon), \quad (39)$$

where  $\mathbf{U} = \mathbf{S}e^{ik\mathbf{L}}$ .

This expansion is absolutely convergent as long as  $\varepsilon > 0$  since the matrix  $\mathbf{U}^n(k + i\varepsilon)$  is then subunitary (all eigenvalues lie within a circle of radius strictly less than 1). As  $\varepsilon \rightarrow 0$ ,  $N^{\text{osc}}(k + i\varepsilon)$  converges to  $N^{\text{osc}}(k)$  pointwise almost everywhere. Moreover,  $|N^{\text{osc}}(k + i\varepsilon)|$  is uniformly bounded by the number of bonds  $B$  (in other systems one can show that the Weyl law implies that  $|N^{\text{osc}}(k)| = O(k^d)$  as  $k \rightarrow \infty$  where  $d$  is the dimension of the system). Therefore,

$$E_c = -\frac{1}{2} \lim_{t \rightarrow 0} \lim_{\varepsilon \rightarrow 0} \int_0^{\infty} (tk - 1) e^{-tk} N^{\text{osc}}(k + i\varepsilon) dk, \quad (40)$$

and, using the convergence of expansion (39),

$$E_c = -\frac{1}{2\pi} \lim_{t \rightarrow 0} \lim_{\varepsilon \rightarrow 0} \sum_{n=1}^{\infty} \frac{1}{n} \text{Im} \int_0^{\infty} (tk - 1) e^{-tk} [\text{tr} \mathbf{U}^n(k + i\varepsilon)] dk. \quad (41)$$

We will now show that the integral

$$R_n = \int_0^{\infty} (tk - 1) e^{-tk} [\text{tr} \mathbf{U}^n(k + i\varepsilon)] dk \quad (42)$$

is absolutely bounded by  $1/n$ . Thus the series is absolutely convergent uniformly in  $\varepsilon$  and  $t$  and we can take the limits inside the sum.

A typical term in the (finite!) expansion of the trace is  $A_p e^{ik\ell_p} e^{-\varepsilon\ell_p}$ . The two exponential factors,  $e^{-tk}$  and  $e^{ik\ell_p}$ , ensure that the integrand is exponentially decaying in  $k$  in the first quadrant of  $\mathbb{C}$ . Therefore we can rotate the contour of integration to the imaginary line,  $k = is$ . The integral becomes

$$R_n = i \int_0^{\infty} (ist - 1) e^{-ist} \text{tr} (\mathbf{S}e^{-(s+\varepsilon)\mathbf{L}})^n ds. \quad (43)$$

We estimate

$$\left| \text{tr} (\mathbf{S}e^{-(s+\varepsilon)\mathbf{L}})^n \right| \leq \sum_{j=1}^{2B} |\lambda_j(s + \varepsilon)|^n, \quad (44)$$

where  $2B$  is the size of the matrix  $\mathbf{S}$  and  $\lambda_j$  is  $j$ -th eigenvalue of the matrix  $\mathbf{S}e^{-(s+\varepsilon)\mathbf{L}}$ . According to a familiar argument (see, e.g. [35]), the maximal  $|\lambda_j|$  is bounded from above

by the maximal singular value of the matrix. The singular values are square roots of the eigenvalues of

$$(\mathbf{S}e^{-(s+\epsilon)\mathbf{L}})^\dagger (\mathbf{S}e^{-(s+\epsilon)\mathbf{L}}) = e^{-2(s+\epsilon)\mathbf{L}},$$

which is a diagonal matrix with the maximal entry  $e^{-2(s+\epsilon)L_{\min}}$  ( $L_{\min}$  is the smallest bond length of the graph). Thus we can estimate

$$\left| \text{tr} (\mathbf{S}e^{-(s+\epsilon)\mathbf{L}})^n \right| \leq e^{-nsL_{\min}} 2B. \quad (45)$$

Finally,

$$|R_n| \leq 2B \int_0^\infty |ist - 1| e^{-nsL_{\min}} ds \sim \frac{1}{n}. \quad (46)$$

We notice that the integrand of (43) can be absolutely bounded by  $e^{-ns(L_{\min}-\delta)}$  for arbitrarily small  $\delta$  and sufficiently small  $t$ . Thus, having brought the limits inside the sum, we can use the dominated convergence theorem to bring them inside the integral. Taking the limit  $t \rightarrow 0$  and  $\epsilon \rightarrow 0$  inside integral (43) produces

$$E_c = \frac{1}{2\pi} \sum_{n=1}^\infty \frac{1}{n} \text{Re} \int_0^\infty \text{tr} (\mathbf{S}e^{-s\mathbf{L}})^n ds. \quad (47)$$

Now we expand the trace,

$$\text{tr} (\mathbf{S}e^{-s\mathbf{L}})^n = \sum_{p \in \mathcal{P}_n} A_p e^{-s\ell_p}, \quad (48)$$

and integrate term by term to recover (34).  $\square$

**Remark 2.** The basic idea of the proof, shifting the convergence into the subunitary matrix (see equation (43) and (45)) can also be used to study the convergence of the trace formula itself. This was done in [36].

**Remark 3.** Since  $\mathbf{S}$  is  $k$ -independent, the trace in the integral is real and we do not need to take the real part in equations (33)-(34). Indeed, the following lemma easily follows from the definition of  $\mathbf{S}$  and [20, Prop 2.4] applied to the matrices  $\boldsymbol{\sigma}^{(v)}$ .

**Lemma 1.** *The  $\mathbf{S}$ -matrix of a graph is  $k$ -independent if and only if it satisfies*

$$\mathbf{J}\mathbf{S}\mathbf{J} = \mathbf{S}^\dagger, \quad (49)$$

where  $\mathbf{J}$  is defined by  $J_{\alpha,\beta} = \delta_{\alpha,\bar{\beta}}$  ( $\bar{\beta}$  is the reversal of  $\beta$  as defined in section 2).

Now the complex conjugate of  $\text{tr} (\mathbf{S}e^{-s\mathbf{L}})^n$  is

$$\text{tr} (e^{-s\mathbf{L}}\mathbf{S}^\dagger)^n = \text{tr} (e^{-s\mathbf{L}}\mathbf{J}\mathbf{S}\mathbf{J})^n = \text{tr} (\mathbf{S}\mathbf{J}e^{-s\mathbf{L}}\mathbf{J})^n = \text{tr} (\mathbf{S}e^{-s\mathbf{L}})^n, \quad (50)$$

where we used the fact that the length of a bond is invariant with respect to direction reversal and, therefore,  $\mathbf{J}e^{-s\mathbf{L}}\mathbf{J} = e^{-s\mathbf{L}}$ .

#### 4.4. Derivatives of the vacuum energy

*Proof of differentiability of  $E_c$ .* We differentiate the expression (33) term by term and show that the result is also absolutely convergent. This can be done by using the following bound on the partial derivatives of  $\text{tr}(\mathbf{S}e^{-s\mathbf{L}})^n$ ,

$$\left| \frac{\partial^{m_1} \dots \partial^{m_B}}{\partial L_1^{m_1} \dots \partial L_B^{m_B}} \text{tr}(\mathbf{S}e^{-s\mathbf{L}})^n \right| \leq \frac{2Be^{-snL_{\min}/2}}{(L_{\min}/2)^{|\mathbf{m}|}}. \quad (51)$$

Before proving (51) we note that it implies the following bound,

$$\left| \frac{1}{n} \int_0^\infty \frac{\partial^{m_1} \dots \partial^{m_B}}{\partial L_1^{m_1} \dots \partial L_B^{m_B}} \text{tr}(\mathbf{S}e^{-s\mathbf{L}})^n ds \right| \leq \frac{2B}{n^2(L_{\min}/2)^{|\mathbf{m}|+1}}. \quad (52)$$

Consequently

$$\sum_{n=1}^\infty \frac{1}{n} \int_0^\infty \frac{\partial^{m_1} \dots \partial^{m_B}}{\partial L_1^{m_1} \dots \partial L_B^{m_B}} \text{tr}(\mathbf{S}e^{-s\mathbf{L}})^n ds$$

converges absolutely and we are therefore allowed to differentiate (33) term by term. We conclude that the vacuum energy is  $C^\infty$  as a function of bond lengths.

To prove bound (51) we use the Cauchy integral formula (see, e.g., [37]),

$$\frac{\partial^{m_1} \dots \partial^{m_B}}{\partial L_1^{m_1} \dots \partial L_B^{m_B}} \text{tr}(\mathbf{S}e^{-s\mathbf{L}})^n = \frac{1}{(2\pi)^B} \int_0^{2\pi} \dots \int_0^{2\pi} \frac{\text{tr}(\mathbf{S}e^{-s(\mathbf{L}+\mathbf{R}(\phi))})^n}{R_1^{m_1} \dots R_B^{m_B}} d\phi_1 \dots d\phi_B \quad (53)$$

where  $R_j = r_j e^{i\phi_j}$  and  $\mathbf{R}(\phi) = \text{diag}\{R_1, \dots, R_B, R_1, \dots, R_B\}$ . Let  $\mathbf{A} = \mathbf{S}e^{-s(\mathbf{L}+\mathbf{R})}$ . Since  $\mathbf{S}$  is unitary, we find  $\mathbf{A}^\dagger \mathbf{A} = e^{-s(2\mathbf{L}+\mathbf{R}+\mathbf{R}^\dagger)}$ . The eigenvalues of  $\mathbf{A}$  are bounded by the maximal singular value of  $\mathbf{A}$ ,

$$|\text{eig}(\mathbf{A})| \leq \max_{b=1\dots B} e^{-s(L_b+r_b \cos(\phi_b))}. \quad (54)$$

By choosing the radius  $r_b = L_{\min}/2$  we see that

$$|\text{eig}(\mathbf{A})| \leq \max_{b=1\dots B} e^{-s(L_b-L_{\min}/2)} = e^{-sL_{\min}/2}, \quad (55)$$

and

$$|\text{tr}(\mathbf{S}e^{-s(\mathbf{L}+\mathbf{R}(\phi))})^n| = |\text{tr} \mathbf{A}^n| \leq \sum_{j=1}^{2B} |\text{eig}(\mathbf{A})_j|^n \leq 2Be^{-snL_{\min}/2}. \quad (56)$$

Using this bound in (53) gives

$$\left| \frac{\partial^{m_1} \dots \partial^{m_B}}{\partial L_1^{m_1} \dots \partial L_B^{m_B}} \text{tr}(\mathbf{S}e^{-s\mathbf{L}})^n \right| \leq \frac{1}{(2\pi)^B} \int_0^{2\pi} \dots \int_0^{2\pi} \frac{2Be^{-snL_{\min}/2}}{(L_{\min}/2)^{|\mathbf{m}|}} d\phi_1 \dots d\phi_B \quad (57)$$

which establishes (51).  $\square$

## 5. Method of images expansion and the equivalence of two expansions

We can evaluate the trace of the cylinder kernel  $T(t)$  by constructing the kernel itself. The cylinder kernel,  $T_{bb'}(t; x, y)$  where  $x$  is measured on bond  $b$  and  $y$  on bond  $b'$  satisfies the following equation on each bond  $b$

$$-\frac{\partial^2}{\partial x^2} T_{bb'}(t; x, y) = \frac{\partial^2}{\partial t^2} T_{bb'}(t; x, y) \quad (58)$$

for  $t > 0$ ,  $T_{bb'} \rightarrow 0$  as  $t \rightarrow \infty$ , with boundary conditions (6) with respect to the  $x$  coordinate, and the initial condition  $T_{bb'}(0; x, y) = \delta_{bb'} \delta(x - y)$ . By separating variables in (58) it can be shown that the trace of  $T$  is

$$T(t) \stackrel{\text{def}}{=} \sum_{b=1}^B \int_0^{L_b} T_{bb'}(t; x, x) dx = \sum_n e^{-k_n t}. \quad (59)$$

The corresponding free space kernel (i.e. the solution of equation (58) on the whole real line with the initial condition  $T_0(0; x - y) = \delta(x - y)$ ) is

$$T_0(t; x - y) = \frac{t/\pi}{t^2 + (x - y)^2}. \quad (60)$$

We can apply the method of images (i.e. multiple reflection) to the free space kernel to obtain the kernel on the graph. The cylinder kernel is then written in terms of paths which begin at  $y$  on the bond  $b'$  and end at  $x$  on the bond  $b$  (the details of the construction are given in [22]),

$$\begin{aligned} T_{bb'}(t; x, y) = & \delta_{bb'} T_0(t; x - y) \\ & + \sum_{n=0}^{\infty} \sum_{\mathbf{p} \in \mathbb{P}_n} \left[ A_{b+\mathbf{p}b'} T_0(t; L_b + \ell_{\mathbf{p}} + x - y) + A_{b+\mathbf{p}b'} T_0(t; -\ell_{\mathbf{p}} - x - y) \right. \\ & \left. + A_{b-\mathbf{p}b'} T_0(t; -\ell_{\mathbf{p}} - L_b + x - y) + A_{b-\mathbf{p}b'} T_0(t; L_{b'} + \ell_{\mathbf{p}} + L_b - x - y) \right] \end{aligned} \quad (61)$$

In the above expression, we denote the two directed bonds associated with the undirected bond  $b$  by  $b^+$  and  $b^-$ . The path of topological length  $n$ ,  $\mathbf{p} = (\alpha_1, \dots, \alpha_n)$  is an  $n$  vector of directed bonds and  $\mathbb{P}_n$  is the set of all such paths. The metric length of a path is  $\ell_{\mathbf{p}} = \sum_{j=1}^n L_{\alpha_j}$  and  $A_{\mathbf{p}} = [\mathbf{S}]_{\alpha_n \alpha_{n-1}} \cdots [\mathbf{S}]_{\alpha_3 \alpha_2} [\mathbf{S}]_{\alpha_2 \alpha_1}$  is the stability amplitude of the path. Note that even at the stage represented in (62) we have assumed the matrix  $\mathbf{S}$  is  $k$ -independent.

To obtain the trace, we let  $b = b'$  and  $y = x$ . While this corresponds to ‘‘closing’’ the paths, we do not always get periodic paths in the topological sense of Section 4.1. Indeed, a periodic path would return to the initial point  $x_b$  with the same momentum (or direction), whereas when the paths corresponding to the second and fourth terms of (62) return to  $x_b$ , the momentum has the opposite sign, see Fig. 2. The latter paths we shall call *bounce paths*. The difficulty in the method of images is in the handling of the bounce paths.

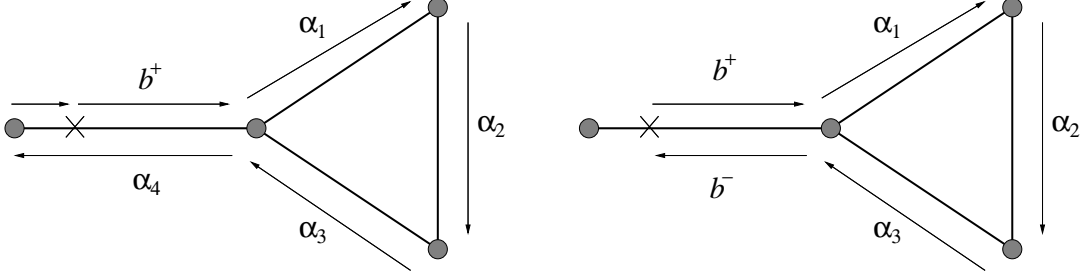


**Figure 2.** An example of a periodic path (left) and a bounce path (right).

After integrating  $T_{bb}(t; x, x)$  we break the formula into three parts

$$T(t) = T_{\text{FS}}(t) + T_{\text{PO}}(t) + T_{\text{BP}}(t), \quad (62)$$

where FS stands for free space, BP for bounce paths, and PO for periodic orbits. The three parts are (taking into account that  $T_0(t; x)$  is even in  $x$ ):

$$T_{\text{FS}}(t) = \sum_{b=1}^B \int_0^{L_b} T_0(t; 0) dx = T_0(t; 0) \mathcal{L}, \quad (63)$$

$$T_{\text{PO}}(t) = \sum_{b=1}^B \int_0^{L_b} \sum_{n=0}^{\infty} \sum_{\mathbf{p} \in \mathbb{P}_n} \left[ A_{b+\mathbf{p}b^+} T_0(t; L_b + \ell_{\mathbf{p}}) + A_{b-\mathbf{p}b^-} T_0(t; \ell_{\mathbf{p}} + L_b) \right] dx, \quad (64)$$

$$T_{\text{BP}}(t) = \sum_{b=1}^B \int_0^{L_b} \sum_{n=0}^{\infty} \sum_{\mathbf{p} \in \mathbb{P}_n} \left[ A_{b+\mathbf{p}b^-} T_0(t; \ell_{\mathbf{p}} + 2x) + A_{b-\mathbf{p}b^+} T_0(t; 2L_b + \ell_{\mathbf{p}} - 2x) \right] dx. \quad (65)$$

We shall use the following lemma to simplify the bounce path term.

**Lemma 2.** *If the scattering matrix  $\mathbf{S}$  of a graph is  $k$ -independent, then*

$$\sum_{\alpha=1}^{2B} A_{\alpha\alpha_{n-1}\dots\alpha_1\bar{\alpha}} = J_{\alpha_1\alpha_{n-1}} A_{\alpha_{n-1}\dots\alpha_1},$$

where  $J_{\alpha,\beta} = \delta_{\alpha,\bar{\beta}}$ .

*Proof.* Writing out the above,

$$\sum_{\alpha} A_{\alpha\alpha_{n-1}\dots\alpha_1\bar{\alpha}} = S_{\alpha_{n-1}\alpha_{n-2}} \cdots S_{\alpha_3\alpha_2} S_{\alpha_2\alpha_1} \sum_{\alpha} S_{\alpha_1\bar{\alpha}} S_{\alpha\alpha_{n-1}}. \quad (66)$$

The last sum in the above is equivalent to an element of  $\mathbf{SJS}$ , but  $\mathbf{JSJS} = \mathbf{I}$ , see lemma 1, and  $\mathbf{J}^{-1} = \mathbf{J}$ , therefore  $\mathbf{SJS} = \mathbf{J}$ .  $\square$

Now we come to the following theorem which proves the equivalence of this method to the trace formula method of Section 4.

**Theorem 2.**

$$T(t) = \frac{\mathcal{L}}{\pi t} + \frac{1}{4} \text{tr} (JS) + \sum_{n=1}^{\infty} \sum_{p \in \mathcal{P}_n} A_p \frac{\ell_p}{n} \frac{t/\pi}{t^2 + \ell_p^2} \quad (67)$$

and consequently,

$$E_c = -\frac{1}{2\pi} \sum_{n=1}^{\infty} \sum_{p \in \mathcal{P}_n} \frac{A_p}{\ell_p n}. \quad (68)$$

**Remark 4.** A special case of this proof was done for the heat kernel with Kirchhoff conditions by Roth [18]. Similarly, Kostykin and Schrader have an analogue of this proof (again, for the heat kernel) in [20].

*Proof.* The first term in  $T(t)$  is the free space term  $T_{\text{FS}}$ , which we found above to be equal to  $T_0(t; 0)\mathcal{L} = \mathcal{L}/\pi t$ . Thus we need only consider the periodic path and bounce path terms.

*Periodic orbit contribution.* There is no  $x$ -dependence in (64), so the integration gives

$$T_{\text{PO}}(t) = \sum_{n=0}^{\infty} \sum_{\mathbf{p} \in \mathbb{P}_n} \sum_{b=1}^B \left[ A_{b-\mathbf{p}b^-} + A_{b+\mathbf{p}b^+} \right] T_0(t; \ell_{\mathbf{p}} + L_b) L_b. \quad (69)$$

The two amplitudes can be written as a single sum over the directed bond  $\alpha$ ,

$$\sum_{b=1}^B \left[ A_{b-\mathbf{p}b^-} + A_{b+\mathbf{p}b^+} \right] T_0(t; \ell_{\mathbf{p}} + L_b) L_b = \sum_{\alpha=1}^{2B} A_{\alpha\mathbf{p}\alpha} T_0(t; \ell_{\mathbf{p}} + L_{\alpha}) L_{\alpha}. \quad (70)$$

The path  $\alpha\mathbf{p}\alpha$  is actually a periodic path of period  $n+1$  which we will denote by  $p$ . The amplitude of  $p$  is  $A_p = A_{\alpha\mathbf{p}\alpha}$  and its length is  $\ell_p = \ell_{\mathbf{p}} + L_{\alpha}$ . Thus,

$$T_{\text{PO}}(t) = \sum_{n=0}^{\infty} \sum_{p \in \mathcal{P}_{n+1}} A_p \frac{\ell_p}{n+1} T_0(t; \ell_p) = \sum_{n=1}^{\infty} \sum_{p \in \mathcal{P}_n} A_p \frac{\ell_p}{n} T_0(t; \ell_p). \quad (71)$$

*Bounce path contribution.* We can again combine the two amplitudes and change the variables in the integrals to obtain

$$T_{\text{BP}}(t) = \frac{1}{2} \sum_{n=0}^{\infty} \sum_{\mathbf{p} \in \mathbb{P}_n} \sum_{\alpha=1}^{2B} A_{\alpha\mathbf{p}\alpha} \int_{\ell_{\mathbf{p}}}^{\ell_{\mathbf{p}}+2L_{\alpha}} T_0(t; x) dx. \quad (72)$$

We now fix  $y > 0$  and introduce the cutoff function,

$$H(y-x) = \begin{cases} 1 & x \leq y \\ 0 & x > y \end{cases}. \quad (73)$$

Instead of  $T_0(t; x)$  in the integral, we consider  $\hat{T}_y(t; x) = T_0(t; x)H(y-x)$ . Since the minimum bond length  $L_{\min}$  is greater than zero, taking  $m$  large enough we will have  $\ell_{\mathbf{p}} > y$  for all



paths of topological length  $m - 1$  or greater. Therefore, for a path  $\mathbf{p}$  in  $\mathbb{P}_{m-1}$  or in  $\mathbb{P}_m$  and any  $\alpha$ , we can write

$$\int_{\ell_{\mathbf{p}}}^{\ell_{\mathbf{p}}+2L_{\alpha}} \hat{T}_y(t; x) dx = \int_{\ell_{\mathbf{p}}}^y \hat{T}_y(t; x) dx, \quad (74)$$

since the integrand is identically zero on both intervals of integration. We can also ignore all paths from  $\mathbb{P}_n$  with  $n > m$ .

We can therefore write the bounce path contribution with the given cutoff in the following form,

$$\begin{aligned} \hat{T}_{\text{BP}}(t) &= \frac{1}{2} \sum_{n=0}^{m-2} \sum_{\mathbf{p} \in \mathbb{P}_n} \sum_{\alpha=1}^{2B} A_{\alpha \mathbf{p} \bar{\alpha}} \int_{\ell_{\mathbf{p}}}^{\ell_{\mathbf{p}}+2L_{\alpha}} \hat{T}_y(t; x) dx \\ &+ \frac{1}{2} \sum_{\mathbf{p} \in \mathbb{P}_{m-1}} \sum_{\alpha=1}^{2B} A_{\alpha \mathbf{p} \bar{\alpha}} \int_{\ell_{\mathbf{p}}}^y \hat{T}_y(t; x) dx + \frac{1}{2} \sum_{\mathbf{p} \in \mathbb{P}_m} \sum_{\alpha=1}^{2B} A_{\alpha \mathbf{p} \bar{\alpha}} \int_{\ell_{\mathbf{p}}}^y \hat{T}_y(t; x) dx. \end{aligned} \quad (75)$$

Applying Lemma 2 to the last set of sums in (75), we obtain

$$\sum_{\mathbf{p} \in \mathbb{P}_m} \sum_{\alpha=1}^{2B} A_{\alpha \mathbf{p} \bar{\alpha}} \int_{\ell_{\mathbf{p}}}^y \hat{T}_y(t; x) dx = \sum_{\mathbf{p} \in \mathbb{P}_{m-2}} \sum_{\beta=1}^{2B} A_{\beta \mathbf{p} \bar{\beta}} \int_{\ell_{\mathbf{p}}+2L_{\beta}}^y \hat{T}_y(t; x) dx. \quad (76)$$

Here the new path is the same as the old path but with the first and the last bond removed and  $\beta$  corresponds to the last bond of the old path.

Now we can take the sum corresponding to  $n = m - 2$  in (75) and add it to the result of (76),

$$\begin{aligned} &\sum_{\mathbf{p} \in \mathbb{P}_{m-2}} \sum_{\alpha=1}^{2B} A_{\alpha \mathbf{p} \bar{\alpha}} \int_{\ell_{\mathbf{p}}}^{\ell_{\mathbf{p}}+2L_{\alpha}} \hat{T}_y(t; x) dx + \sum_{\mathbf{p} \in \mathbb{P}_{m-2}} \sum_{\beta=1}^{2B} A_{\beta \mathbf{p} \bar{\beta}} \int_{\ell_{\mathbf{p}}+2L_{\beta}}^y \hat{T}_y(t; x) dx \\ &= \sum_{\mathbf{p} \in \mathbb{P}_{m-2}} \sum_{\alpha=1}^{2B} A_{\alpha \mathbf{p} \bar{\alpha}} \int_{\ell_{\mathbf{p}}}^y \hat{T}_y(t; x) dx \end{aligned} \quad (77)$$

Therefore,  $\hat{T}_{\text{BP}}(t)$  can be rewritten exactly in the form of (75) but with  $m$  reduced by 1. Proceeding by induction, we obtain

$$\hat{T}_{\text{BP}}(t) = \frac{1}{2} \sum_{\alpha}^{2B} A_{\alpha \bar{\alpha}} \int_0^y \hat{T}(t; x, y) dx + \frac{1}{2} \sum_{\alpha=1}^{2B} J_{\alpha \alpha} \int_{L_{\alpha}}^y \hat{T}(t; x, y) dx. \quad (78)$$

However,  $J_{\alpha \alpha} = 0$  and we can take the limit  $y \rightarrow \infty$  to get back  $T_{\text{BP}}(t)$ ,

$$T_{\text{BP}}(t) = \frac{1}{2} \left[ \sum_{\alpha=1}^{2B} (\mathbf{S}\mathbf{J})_{\alpha \alpha} \right] \int_0^{\infty} T_0(t; x) dx = \frac{1}{4} \text{tr}(\mathbf{S}\mathbf{J}). \quad (79)$$

The significance on this term is explored thoroughly in [38]. Since it is constant it vanishes upon differentiation and thus makes no contribution to the vacuum energy expression.  $\square$

The above method can be applied to other integral kernels, and we can also find the vacuum energy density if we look at  $-\frac{1}{2}\frac{\partial}{\partial t}T_{bb}(t; x, x)$ , see [22].

## 6. Random matrix models of vacuum energy

It has been observed by Fulling [23, 6] that level repulsion tends to decrease the magnitude of vacuum energy. A natural conclusion would be that in a chaotic system the vacuum energy should be suppressed. In this section we attempt to quantify and model this observation.

The first serious problem is that of comparison: vacuum energy should be suppressed compared to what? One cannot directly compare vacuum energy of a chaotic system to that of an integrable one: such systems would be too different. Thus the right approach seems to be the average of the energy over an appropriate ensemble of chaotic/integrable systems

In such situations it is customary to employ random matrices as models of chaotic systems. Which leads to a second problem: vacuum energy is not an exciting quantity when the spectrum is finite. Thus, (finite) random matrices do not immediately provide a suitable model.

In this section we use a fusion of random matrix and graph models as a testing ground for the above conjecture. Namely, we study quantum graphs with equal bond lengths but with scattering matrices drawn from the appropriate ensembles of unitary matrices. The advantages are clear: each individual system will have an infinite spectrum, the spectra (in the limit of large graphs) will have the desired statistics and the averaging can be done explicitly.

### 6.1. Average vacuum energy

The spectrum of a generic quantum system with a chaotic classical counterpart is observed to behave like that of a random matrix, which is referred to as the Bohigas-Giannoni-Schmit conjecture [39]. For a system with time-reversal symmetry the appropriate ensemble of unitary matrices is the circular orthogonal ensemble (COE) while in the absence of time-reversal symmetry it is the circular unitary ensemble (CUE), which is the unitary group  $U(N)$  with Haar measure see [40]. For a system with time-reversal symmetry and half-integer spin the random matrix should be drawn from the circular symplectic ensemble (CSE). To model the vacuum energy of a generic chaotic system we consider quantum graphs with equal bond lengths where the scattering matrix  $\mathbf{S}$  is taken from an appropriate ensemble. In drawing  $\mathbf{S}$  from a random matrix ensemble we must first assume that the random matrix models a graph which allows scattering between all the edges, in other words a rose graph where one central vertex connects  $B$  loops. A random matrix  $\mathbf{S}$  will also not, in general, correspond to scattering amplitudes accessible from matching conditions of a self-adjoint Laplace operator. However, both these limitations seem to be intrinsic to any random matrix model. Our model

should therefore only be regarded as a way to investigate average properties of vacuum energy when its generating spectrum has the desired random matrix level repulsion.

The average vacuum energy of such a model can be evaluated using equation (22), which expresses the vacuum energy of a graph with equal bond lengths in terms of the eigenphases of  $\mathbf{S}$ . Using the standard expression for the eigenphase density of the random matrices results in

$$\langle E_c \rangle_\beta = -\frac{\pi}{L} \frac{1}{\mathcal{N}_\beta} \int_0^{2\pi} \dots \int_0^{2\pi} \sum_{j=1}^{2B} B_2(\theta_j/2\pi) \prod_{l < m} \left| 2 \sin \left( \frac{\theta_l - \theta_m}{2} \right) \right|^\beta d\theta_1 \dots d\theta_{2B} = 0 \quad (80)$$

where  $\mathcal{N}_\beta$  is a normalization constant and  $\beta = 1$  for the COE,  $\beta = 2$  for the CUE and  $\beta = 4$  for CSE.

The eigenphases of an integrable system, in contrast, behave like uniformly distributed random numbers on the interval  $[0, 2\pi]$ . This can also be modeled by integrating the vacuum energy expression, equation (22), over  $2B$  independent uniform random phases,

$$\langle E_c \rangle_{\text{Poisson}} = -\frac{\pi}{L} \frac{1}{(2\pi)^{2B}} \int_0^{2\pi} \dots \int_0^{2\pi} \sum_{j=1}^{2B} B_2(\theta_j/2\pi) d\theta_1 \dots d\theta_{2B} = 0. \quad (81)$$

In each case the average  $\langle E_c \rangle$  of the vacuum energy is zero. In fact, the vacuum energy expression must be zero when averaged over any measure which is invariant under a rotation of all the eigenphases by some angle  $\gamma$ . Indeed, in Section 4.2 we have shown that

$$E_c = -\frac{1}{\pi L} \sum_{n=1}^{\infty} \frac{1}{2n^2} (\text{tr} \mathbf{S}^n + \text{tr}(\mathbf{S}^\dagger)^n). \quad (82)$$

But for any rotationally invariant distribution of eigenphases on the unit circle,  $\langle \text{tr} \mathbf{S}^n \rangle = 0$  for all  $n > 0$  and thus the mean vacuum energy is always zero. As the Casimir force is the derivative of  $E_c$  with respect to  $L$  this suggests that there is no *a priori* reason to expect either an attractive or repulsive force based purely on the underlying nature of the classical dynamics.

## 6.2. Variance

To get a handle on how the magnitude of the vacuum energy is affected by the distribution of the eigenvalues we will calculate the variance of the vacuum energy for the ensembles of random graphs introduced previously. For Poisson distributed eigenphases the variance is

$$\begin{aligned} \langle E_c^2 \rangle_{\text{Poisson}} &= \frac{\pi^2}{L^2} \frac{1}{(2\pi)^{2B}} \int_0^{2\pi} \dots \int_0^{2\pi} \sum_{j=1}^{2B} B_2^2(\theta_j/2\pi) d\theta_1 \dots d\theta_{2B} \\ &= \frac{\pi^2 B}{90L^2}, \end{aligned} \quad (83)$$

where  $2B$  is the dimension of  $\mathbf{S}$  and we used the independence of  $\theta_j$  to conclude that

$$\langle B_2(\theta_r/2\pi) B_2(\theta_j/2\pi) \rangle = \langle B_2(\theta_r/2\pi) \rangle \langle B_2(\theta_j/2\pi) \rangle = 0. \quad (84)$$

The variance of the vacuum energy modeled by random matrices from the circular ensembles can be computed using expression (30),

$$\langle E_c^2 \rangle = \frac{1}{\pi^2 L^2} \sum_{m,n=1}^{\infty} \frac{1}{4n^2 m^2} \langle (\text{tr } \mathbf{S}^n + \text{tr}(\mathbf{S}^\dagger)^n) (\text{tr } \mathbf{S}^m + \text{tr}(\mathbf{S}^\dagger)^m) \rangle. \quad (85)$$

For the circular ensembles  $\langle \text{tr } \mathbf{S}^n \text{tr}(\mathbf{S}^\dagger)^m \rangle = 0$  unless  $m = n$  as the average of a product of matrix elements is zero unless the number of elements of the matrix and the number from its Hermitian conjugate are the same [41]. Consequently

$$\langle E_c^2 \rangle = \frac{1}{2\pi^2 L^2} \sum_{n=1}^{\infty} \frac{1}{n^4} \langle |\text{tr } \mathbf{S}^n|^2 \rangle. \quad (86)$$

We notice that  $\langle |\text{tr } \mathbf{S}^n|^2 \rangle$  is the form factor of the (finite) ensemble and use the standard formulae [40] for CUE

$$\langle |\text{tr } \mathbf{S}^n|^2 \rangle_{\text{CUE}} = \begin{cases} (2B)^2 & n = 0 \\ n & |n| < 2B \\ 2B & |n| \geq 2B \end{cases} \quad (87)$$

to obtain

$$\langle E_c^2 \rangle_{\text{CUE}} = \frac{1}{2\pi^2 L^2} \left( \frac{1}{2} \Psi^{(2)}(2B) + \zeta(3) + \frac{B}{3} \Psi^{(3)}(2B) \right) \quad (88)$$

where  $\Psi^{(n)}(x)$  is the  $n$ -th polygamma function and  $\zeta$  the Riemann zeta function. For all fixed  $B$  this is less than  $\pi^2 B/360$  the variance of the Poisson distributed eigenphases. In fact

$$\lim_{B \rightarrow \infty} \langle E_c^2 \rangle_{\text{CUE}} = \frac{\zeta(3)}{2\pi^2 L^2}. \quad (89)$$

This result parallels that for a random matrix model of the grand potential considered in [16]. Thus, while the variance of the Poisson ensemble grows linearly with matrix size, the CUE variance converges.

The relevant parts of the form factor of the COE and CSE for finite matrix size are,

$$\langle |\text{tr } \mathbf{S}^n|^2 \rangle_{\text{COE}} = \begin{cases} 2n - n \sum_{m=1}^n \frac{1}{m+(2B-1)/2} & 0 < n \leq 2B \\ 4B - n \sum_{m=1}^{2B} \frac{1}{m+n-(2B+1)/2} & 2B \leq n \end{cases} \quad (90)$$

$$\langle |\text{tr } \mathbf{S}^n|^2 \rangle_{\text{CSE}} = \begin{cases} 2n + n \sum_{m=1}^n \frac{1}{(2B+1)/2-m} & 0 < n \leq 2B \\ 4B & 2B \leq n \end{cases} \quad (91)$$

Note that in the CSE form factor the double degeneracy of the eigenphases of  $\mathbf{S}$  (Kramers' degeneracy) has not been lifted. Using (86) we evaluate

$$\langle E_c^2 \rangle_{\text{COE}} = \frac{1}{\pi^2 L^2} \left( \left( \frac{1}{2} \Psi^{(2)}(2B) + \zeta(3) \right) \left( 1 + \frac{1}{2} \Psi(B+1/2) \right) - \sum_{n=1}^{2B-1} \frac{\Psi(n+B+1/2)}{2n^3} \right) \quad (92)$$

$$+ \sum_{n=2B}^{\infty} \left[ \frac{2B}{n^4} + \frac{\Psi(n-B+1/2) - \Psi(n+B-1/2)}{2n^3} \right] \quad (93)$$

$$\langle E_c^2 \rangle_{\text{CSE}} = \frac{1}{\pi^2 L^2} \left( \left( \frac{1}{2} \Psi^{(2)}(2B) + \zeta(3) \right) \left( 1 + \frac{1}{2} \Psi(1/2 - B) \right) \right) \quad (94)$$

$$- \sum_{n=1}^{2B-1} \frac{\Psi(n - B + 1/2)}{2n^3} + \frac{B}{3} \Psi^{(3)}(2B) \right) \quad (95)$$

For  $B > 1$   $\langle E_c^2 \rangle_{\text{COE}}$  and  $\langle E_c^2 \rangle_{\text{CSE}}$  are less than  $\langle E_c^2 \rangle_{\text{Poisson}}$ .

While the results do not have a simple closed form, in the limit of large matrices the result is rather concise,

$$\lim_{B \rightarrow \infty} \langle E_c^2 \rangle_{\text{COE}} = \frac{\zeta(3)}{\pi^2 L^2} = \lim_{B \rightarrow \infty} \langle E_c^2 \rangle_{\text{CSE}} \quad (96)$$

Modeling the vacuum energy variance of a quantum graph through random matrices suggests that the magnitude of the vacuum energy where eigenphases of  $\mathbf{S}$  experience level repulsion are indeed smaller on average than those where the eigenphases are Poisson distributed. Moreover, the magnitude gets smaller as the level repulsion increases from linear (COE) to quadratic (CUE) and quartic (CSE). Indeed, to compare the effect of the increased level repulsion in CSE we need to lift the Kramers' degeneracy: otherwise the degeneracy "compensates" the repulsion. Without the degeneracy, the result for CSE becomes 4 times smaller:

$$\lim_{B \rightarrow \infty} \langle E_c^2 \rangle_{\text{CSE}/\text{Kramers}} = \frac{\zeta(3)}{4\pi^2 L^2},$$

thus leading to

$$\langle E_c^2 \rangle_{\text{COE}} > \langle E_c^2 \rangle_{\text{CUE}} > \langle E_c^2 \rangle_{\text{CSE}/\text{Kramers}}$$

for  $B > 1$ .

## 7. Conclusions

Through both the method of images and the trace formula, we demonstrate that the vacuum energy in quantum graphs is a well-defined quantity (i.e. it is both convergent and a smooth function of the bond lengths). The closed form expression (5) is dependent only on the periodic paths in the quantum graph; this is a consequence of the exactness of the trace formula which includes only those paths. Having demonstrated how the bounce paths (closed paths that are not periodic) cancel when using the method of images we hope that our proof will shed light on the observation that periodic paths provide the correct leading asymptotic behavior even when the trace formula is only semiclassically correct.

The smoothness of the expression for the vacuum energy in a quantum graph allows us to suggest an alternative method for its calculation, by approximating with systems with simpler geometries. In the case of graphs the "simpler geometry" means rational bond lengths, where an explicit expression for the vacuum energy is obtained.

We also suggest a random ensemble model for the vacuum energy when the statistics of the spectrum are Poisson (for integrable systems) or random matrix (for chaotic systems). We find the average energy in both cases to be zero, thus giving no *a priori* reason to expect a positive or negative energy from the dynamics. Furthermore, we find the variance of the energy and conclude that the magnitude of the energy is typically smaller when the level repulsion is stronger. We stress that this prediction is only correct in the probabilistic sense and no conclusions about particular systems can yet (if ever!) be drawn.

## Acknowledgments

The authors would like to thank S.A. Fulling, J.P. Keating, K. Kirsten, P. Kuchment, M. Pivarsky and B. Winn for their helpful comments. This material is based upon work supported by the National Science Foundation under Grants No. DMS-0604859, PHY-0554849 and DMS-0648786. The authors would also like to thank the Isaac Newton Institute for Mathematical Sciences, Cambridge, UK, where part of the research took place.

## References

- [1] Casimir H B. On the attraction between two perfectly conducting plates. *Proc. K. Ned. Akad. Wetensch.*, 51:793–795, 1948.
- [2] Boyer T H. Quantum zero-point energy and long-range forces. *Ann. Phys.*, 56:474–503, February 1970.
- [3] Plunien G, Müller B, and Greiner W. The Casimir effect. *Phys. Rep.*, 134:87–193, March 1986.
- [4] Bordag M, Mohideen U, and Mostepanenko V M. New developments in the Casimir effect. *Phys. Repts.*, 353:1–205, 2001.
- [5] Milton K A. The Casimir effect: recent controversies and progress. *J. Phys. A*, 37(38):R209–R277, 2004.
- [6] Fulling S A. Global and local vacuum energy and closed orbit theory. In Milton K, editor, *Proceedings of the 6th Workshop on Quantum Field Theory under the Influence of External Conditions (Norman, OK, Sept. 2003)*, pages 166–174. Rinton Press, 2004.
- [7] Cavalcanti R M. Casimir force on a piston. *Phys. Rev. D*, 69(6):065015, March 2004.
- [8] Fulling S A, Kaplan L, and Wilson J H. Vacuum energy and repulsive Casimir forces in quantum star graphs. *Phys. Rev. A*, 76, 2007. [arXiv:quant-ph/0703248v1](https://arxiv.org/abs/quant-ph/0703248v1).
- [9] Brown L S and Maclay G J. Vacuum stress between conducting plates: An image solution. *Physical Review*, 184:1272–1279, August 1969.
- [10] Jaekel M T and Reynaud S. Casimir force between partially transmitting mirrors. *J. Physique I*, 1:1395–1409, 1991.
- [11] Schaden M and Spruch L. Infinity-free semiclassical evaluation of Casimir effects. *Phys. Rev. A*, 58:935–953, August 1998.
- [12] Fulling S A. Periodic orbits, spectral oscillations, scaling, and vacuum energy: beyond HaMiDeW. In *Proceedings of the International Meeting on Quantum Gravity and Spectral Geometry, (Naples, 2001)*, volume 104, pages 161–164. Nucl. Phys. B (Proc. Suppl.), 2002.
- [13] Jaffe R L and Scardicchio A. Casimir effect and geometric optics. *Phys. Rev. Lett.*, 92(7):070402, February 2004.

- [14] Liu Z H and Fulling S A. Casimir energy with a Robin boundary: the multiple-reflection cylinder-kernel expansion. *New Journal of Physics*, 8(10):234, 2006.
- [15] Martin S. Sign and other aspects of semiclassical Casimir energies. *Phys. Rev. A*, 73(4):042102, 2006.
- [16] Leboeuf P, Monastra A G, and Bohigas O. The Riemannium. *Regul. Chaotic Dyn.*, 6(2):205–210, 2001.
- [17] Gnuzmann S and Smilansky U. Quantum graphs: Applications to quantum chaos and universal spectral statistics. *Advances in Physics*, 55(5):527–625, 2006.
- [18] Roth J P. Le spectre du Laplacien sur un graphe. In Mokobodzki G and Pinchon D, editors, *Théorie du potentiel*, Proceedings of the Colloque Jacques Deny, Orsay 1983, Lecture Notes in Mathematics. Springer, June 1985.
- [19] Kottos T and Smilansky U. Quantum chaos on graphs. *Phys. Rev. Lett.*, 79:4794–4797, December 1997.
- [20] Kostrykin V, Potthoff J, and Schrader R. Heat kernels on metric graphs and a trace formula. In Germinet F and Hislop P D, editors, *Adventures in mathematical physics*, volume 447 of *Contemporary mathematics*, pages 175–198. AMS, 2007.
- [21] Winn B. On the trace formula for quantum star graphs. In G. Berkolaiko, R. Carlson, S. Fulling, and P. Kuchment, editors, *Proceedings of Joint Summer Research Conference on Quantum Graphs and Their Applications, 2005*, pages 293–307. AMS, 2006.
- [22] Wilson J H. Vacuum energy in quantum graphs. Undergraduate Research Fellow Thesis, Texas A&M University. <http://handle.tamu.edu/1969.1/5682>, 2007.
- [23] Fulling S A. private communication, 2003.
- [24] Fulling S A. Local spectral density and vacuum energy near a quantum graph vertex. In G. Berkolaiko, R. Carlson, S. Fulling, and P. Kuchment, editors, *Proceedings of Joint Summer Research Conference on Quantum Graphs and Their Applications, 2005*, pages 161–172. AMS, 2006.
- [25] Bellazzini B and Mintchev M. Quantum fields on star graphs. *J. Phys. A*, 39(35):11101–11117, 2006.
- [26] Kuchment P. Quantum graphs: I. some basic structures. *Waves in Random Media*, 14:S107–S128, January 2004.
- [27] Kostrykin V and Schrader R. Kirchhoff’s rule for quantum wires. *J. Phys. A*, 32(4):595–630, 1999.
- [28] Kostrykin V and Schrader R. Kirchhoff’s rule for quantum wires. ii: The inverse problem with possible applications to quantum computers. *Fortschritte der Physik*, 48:703–716, 2000.
- [29] Kostrykin V and Schrader R. The generalized star product and the factorization of scattering matrices on graphs. *Journal of Mathematical Physics*, 42:1563–1598, April 2001.
- [30] Kottos T and Smilansky U. Periodic orbit theory and spectral statistics for quantum graphs. *Ann. Phys.*, 274:76–124, 1999.
- [31] von Below J. A characteristic equation associated to an eigenvalue problem on  $c^2$ -networks. *Linear Algebra Appl.*, 71:309–325, 1985.
- [32] Schanz H and Smilansky U. Spectral statistics for quantum graphs: periodic orbits and combinatorics. *Phil. Mag. B*, page 19992021, 2000. Proceedings of the Australian summer school on quantum chaos and mesoscopics.
- [33] Tanner G. Unitary stochastic matrix ensembles and spectral statistics. *J. Phys. A: Math. Gen.*, 34:8485–8500, 2001.
- [34] Abramowitz M and Stegun I A. *Handbook of Mathematical Functions*. Dover, New York, 1964.
- [35] Weyl H. Inequalities between the two kinds of eigenvalues of a linear transformation. *Proc. Nat. Acad. Sci. U. S. A.*, 35:408–411, 1949.
- [36] Winn B. A conditionally convergent trace formula for quantum graphs. Submitted to the proceeding of Isaac Newton Institute program “Analysis on Graphs and its Applications”, 2007.
- [37] Mathews J and Walker R L. *Mathematical Methods of Physics*. Addison-Wesley, 1970.
- [38] Fulling F, Kuchment P, and Wilson J H. Index theorems for quantum graphs. *J. Phys. A: Math. Theor.*, 40:14165–14180, 2007.

- [39] Bohigas O, Giannoni M-J, and Schmit C. Characterization of chaotic quantum spectra and universality of level fluctuation laws. *Phys. Rev. Lett.*, 52:1–4, 1984.
- [40] Haake F. *Quantum Signatures of Chaos*. Springer, 2 edition, June 2006.
- [41] Brouwer P W and Beenakker C W J. Diagrammatic method of integration over the unitary group, with applications to quantum transport in mesoscopic systems. *J. Math. Phys.*, 37:4904–4934, 1996.